Trajectory Planning for Mobile Manipulators with Control Constraints

Grzegorz Pająk, Iwona Pająk
University of Zielona Góra, Institute of Mechanical Engineering, prof. Z. Szafrana 4, 65-516 Zielona Góra, Poland

Abstract: This paper presents the method of trajectory planning for mobile manipulators considering limitations resulting from capabilities of robotic system actuators. The fulfillment of control constraints is achieved by introducing virtual control scaling of the robot trajectory in the limited periods of time. Such an approach allows researchers to obtain the trajectories fulfilling control constraints without significantly increasing the time of task execution. The proposed method generates sub-optimal trajectories maximizing the manipulability measure of the robot arm, preserves mechanical and collision avoidance limitations and can be used in real-time trajectory planning. The effectiveness of the presented solution is confirmed by computer simulations involving a mobile manipulator with parameters corresponding to KUKA youBot.

Keywords: mobile robots, trajectory planning, state constraints, control constraints, obstacle avoidance

1. Introduction

In the presented work the problem of trajectory planning for mobile manipulators consisting of a nonholonomic platform and a holonomic arm is considered. The task of this type requires a number of limitations to be considered resulting from the nature of the robot task, its mechanical construction and the presence of the obstacles in the workspace. In the literature several approaches to solving such a problem have been presented. Some of the solutions omit dynamic parameters of the robot, however, the algorithms taking into account the dynamics of the system seem to be more interesting. Such methods can be divided into two groups: in the first one the manipulator arm and the platform are treated as two separate subsystems, in the other group the whole robot is considered as one integrated system.

The solution based on the decomposition of the task into two independent sub-tasks has been proposed by [14]. In this approach the effector follows the path described relative to the base and the platform moves along a certain flat curve. The proposed solution leads to a system with two controllers: the kinematic controller enables tracking the path by both subsystems and the dynamic one ensures the convergence of the robot velocities to velocities obtained from the kinematic controller. A similar approach, using the decentralized control for the task of tracing the end-effector trajectory, was also described by [4] and [23]. The solution of the task for mobile robot moving between initial and final configurations provided in a complex environment has been presented in [13]. The authors have focused on planning the shortest collision-free trajectory, they have not considered state and control constraints and have obtained smooth trajectories using cubic polynomials.

In addition to solutions where the arm and the platform are treated as separate subsystems, there are also approaches where the mobile manipulator is considered as one integrated system. Such a solution for mobile manipulators operating in a limited workspace has been presented by [8]. The authors have paid particular attention to maintaining the stability of the system by the appropriate coordination of the movements of the platform and the manipulator. An approach that integrates motion planning with the control of the mobile manipulator as well as control of the nonholonomic trolley has been suggested by [21]. Article [6] has offered a class of controllers solving the trajectory tracking problem subject to control-dependent constraints. The trajectory of the robot has been determined in such a way as to minimize the instantaneous energy and provide collision-free motion. In [18] the authors have used attractive and repulsive potential functions to plan the trajectory of the mobile manipulator equipped with a car-like platform. The proposed method enables planning the collision-free motion between initial and final positions, taking into account mechanical singularities and velocity limitations, still the dynamics of this system is not considered. The Simulated Annealing algorithm has been applied in [1] to solve the time optimal trajectory planning task. The author has focused on maximizing the reachability of the target point introducing a new singularity avoidance metric named Manipulability Percentage Index. The limitations on generalized coordinates, velocities and accelerations have been analyzed, but control constraints have not been considered. A systematic review of motion planning approaches of mobile manipulators has been undertaken by [19].

Autor korespondujący:
Grzegorz Pająk, g.pajak@iim.uz.zgora.pl

Artykuł recenzowany
nadesłany 19.02.2023 r., przyjęty do druku 05.04.2023 r.

In the method of trajectory planning outlined in this paper the mobile manipulator is treated as one integrated system. The presented approach solves the point-to-point trajectory planning problem and takes into account both state and control constraints, moreover, it provides a sub-optimal solution, minimizing the instantaneous manipulability measure dependent index. As a result, the method generates the trajectories which avoid singular configurations and provides high manipulability measure of the manipulator arm. Such an approach can be utilized to plan the trajectory of industrial mobile robots moving between multiple production workstations as well as space rovers equipped with a robotic arm. One of the typical task of such rovers is to move to the selected location to collect samples or take photos of the object specified by the operator. It seems that the method taking into account state and control constraints, the manipulability of the arm and collision avoidance conditions is suitable to plan the motion of such robots in these cases.

As opposed to similar approaches, the method suggested in this paper incorporates nonholonomic constraints in a Pfaffian form explicitly to the control algorithm, so it does not require transformation to a driftless control system. The effectiveness of the proposed algorithm allows it to be used in real-time trajectory planning. The solution of the primary robot task utilizes an extended Jacobian approach and it is based on previous works by the authors [16, 17], still the new approach considering the limitations resulting from physical abilities of actuators is put forward in this paper. In contrast to the works cited, where the fulfillment of controls limitations was achieved by scaling the whole robot trajectory, in this paper scaling is applied in certain time periods only.

As described in Section 4 such a novel approach significantly improves the efficiency of the proposed algorithm as it does not significantly extend the time needed to complete the task, which was the biggest disadvantage of earlier solutions. Moreover, in this paper the condition for the existence of the solution in the presence of control limitations is formulated.

2. Problem formulation

In this paper the mobile manipulator composed of the nonholonomic platform and the holonomic arm is considered. Introducing n_p-elemental vector q_p consisting of configuration coordinates of the platform and n_a-elemental vector q_a including configuration coordinates of the arm, the mobile manipulator can be described by the n-elemental vector ($n = n_p + n_a$) of generalized coordinates in the form

$$q = \begin{bmatrix} q_p^{\mathrm{T}} & q_a^{\mathrm{T}} \end{bmatrix}^{\mathrm{T}}. \tag{1}$$

The task of the mobile robot is to move its end-effector to the specified location in the m-dimensional workspace. Such tasks are performed when the robot moves to another location to accomplish a specific task or transport an object held by its gripper. In such a case, it is assumed that at the initial time $t = 0$ the robot is in a certain configuration $q(0) = q_0$, which was achieved following the completion of the previous operation. The task is thus to find the trajectory $q(t)$ ensuring, at the final moment $t = T$, reaching the final unknown configuration $q(T) = q_T$, allowing to achieve the desired end-effector location p_f

$$k(q(T)) - p_f = 0, \tag{2}$$

where $k : \mathfrak{R}^n \to \mathfrak{R}^m$ denotes m-dimensional mapping describing the position and orientation of the robot end-effector in the workspace.

It is assumed that the initial configuration q_0 is non-singular and collision free, moreover the mobile manipulator is motionless at the initial and final moment of the motion:

$$\dot{q}(0) = 0, \quad \dot{q}(T) = 0. \tag{3}$$

The robot motion is subject to various constraints. Due to nonholonomic of the platform its movement is limited by h phase constraints described in the Pfaffian form

$$A\left(q_p\right)\dot{q}_p = 0, \tag{4}$$

where: A is ($h \times n_p$) the Pfaffian full rank matrix.

The arm of the mobile robot should avoid singular configurations in which it loses its manipulative abilities. Hence, in this work, the maximization of manipulability measure was put forward. In this case, the manipulability of the holonomic arm is determined using the index based on [22] in the form

$$\mu\left(q_a\right) = \sqrt{\det\left(J_a\left(q_a\right)J_a^{\mathrm{T}}\left(q_a\right)\right)}, \tag{5}$$

where matrix $J_a\left(q_a\right) = \partial k(q)/\partial q_a$ is the analytical Jacobian of the manipulator arm.

Additionally, due to mechanical limitations and constraints related to obstacles existing in the workspace, robot motion is limited by state inequality constraints in the form of

$$\forall t \in \left[0, T\right] \quad C_M^i\left(q(t)\right) \ge 0, \quad i = 1, \ldots, L_M \tag{6}$$

$$\forall t \in \left[0, T\right] \quad C_O^i\left(q(t)\right) \ge 0, \quad i = 1, \ldots, L_O \tag{7}$$

where L_M and L_O denote a total number of mechanical and collision avoidance constraints, C_M^i and C_O^i describe the algebraic distance of the i-th configuration from its limits and algebraic distance of the robot from i-th obstacle, respectively.

Moreover, the physical abilities of robot actuators imply the need of consideration of constraints connected to controls. It is a very important issue from a practical point of view, yet it significantly complicates the solution of the task. In the case of nonholonomic mobile manipulators, an additional problem related to the description of dynamics and the need to take into account the restrictions on platform movement needs to be considered. On the other hand, neglecting these limitations can lead to a solution which can be impossible to adopt by a real robot. Such constraints can be described in the general form as a set of ($n - h$) inequalities as

$$\forall t \in \left[0, T\right] \quad \tau_{\min}^i \le \tau^i(t) \le \tau_{\max}^i, \quad i = 1, \ldots, (n-h) \tag{8}$$

where $\tau = \left[\tau^1 \ldots \tau^{n-h}\right]^{\mathrm{T}}$ is the vector of control (torques/forces) and $\tau_{\min} = \left[\tau_{\min}^1 \ldots \tau_{\min}^{n-h}\right]^{\mathrm{T}}$, $\tau_{\max} = \left[\tau_{\max}^1 \ldots \tau_{\max}^{n-h}\right]^{\mathrm{T}}$ are lower and upper limits on τ.

3. Trajectory planning

3.1. Point-to-point trajectory planning

In order to solve the basic task of the robot (2), taking into account constraints (3) and (7) the approach based on the method presented by the authors in [16] and [17] was applied. Due to the redundancy of the mobile manipulator considered in this work, the presented solution uses an extended Jacobian approach making it possible to take into account additional conditions specifying the way of task execution. To this purpose, additional criteria in the following form are introduced

$$H(q) = -\mu(q_a) + \sum_{i=1}^{L_M} \kappa_M^i \left(C_M^i(q)\right), \tag{9}$$

where $\kappa_M^i(\cdot)$ is any internal penalty function tending to infinity if the configuration approaches i-th limit.

The minimization of criteria (9) allows for the determination of the configuration maintaining the high dexterity of the arm (maximizing the index (5)) and satisfying mechanical limitations (6). Following the derivation method presented in [17] and introducing the Jacobian of the mobile manipulator as $((m + h) \times n)$ dimensional matrix in the form of

$$\mathcal{J}(q) = \left[J^{\mathrm{T}}(q), \quad \mathcal{A}^{\mathrm{T}}(q)\right]^{\mathrm{T}}. \tag{10}$$

where $J(q) = \partial k(q)/\partial q$, $\mathcal{A} = \left[A(q)\ 0\right]$, the necessary condition of the minimum of criteria (9) can be determined. Finally, the condition introducing additional $(n - m - h)$ dependencies, supplementing the basic task of the robot and allowing to create the extended Jacobian, can be determined as

$$H_{q,F}(q) - \left(\mathcal{J}_R^{-1}(q)\mathcal{J}_F(q)\right)^{\mathrm{T}} H_{q,R}(q) = 0, \tag{11}$$

where $H_q(q) = \partial H(q)/\partial q$, $\mathcal{J}_R$ is a square matrix constructed from $(m + h)$ linear independent columns of $\mathcal{J}$, $\mathcal{J}_F$ is a matrix obtained by excluding $\mathcal{J}_R$ from $\mathcal{J}$ and $H_{q,F}$, $H_{q,R}$ are vectors containing the elements of H_q corresponding to columns of the matrix $\mathcal{J}_R$, $\mathcal{J}_F$, respectively.

Using the dependency (11) the mapping $e(q,\dot{q})$, determining the distance between the current configuration $q(t)$ and the permitted (non-singular, satisfying mechanical constraints) unknown final configuration q_T, can be recorded as

$$e(q,\dot{q}) = \begin{bmatrix} k(q) - p_f \\ H_{q,F}(q) - \left(\mathcal{J}_R^{-1}(q)\mathcal{J}_F(q)\right)^{\mathrm{T}} H_{q,R}(q) \\ \mathcal{A}(q)\dot{q} \end{bmatrix}. \tag{12}$$

Introducing mappings e_I and e_{II} constructed from the components of e in the following form

$$\begin{gathered} e_I(q) = \begin{bmatrix} k(q) - p_f \\ H_{q,F}(q) - \left(\mathcal{J}_R^{-1}(q)\mathcal{J}_F(q)\right)^{\mathrm{T}} H_{q,R}(q) \end{bmatrix}, \\ e_{II}(q,\dot{q}) = \mathcal{A}(q)\dot{q}, \end{gathered} \tag{13}$$

the dependencies specifying the trajectory of the robot to the final location p_f satisfying constraints (3), (7) and maximizing the manipulability measure (5) are put forward as the following system of differential equations

$$\begin{aligned} \ddot{e}_I(q,\dot{q},\ddot{q}) + \Lambda_{V_I}\dot{e}_I(q,\dot{q}) + \Lambda_{P_I}e_I(q) &= 0 \\ \dot{e}_{II}(q,\dot{q},\ddot{q}) + \Lambda_{II}e_{II}(q,\dot{q}) &= 0 \end{aligned} \tag{14}$$

where $\Lambda_{V_I} = \mathrm{diag}\left\{\Lambda_{V_I}^1, \ldots, \Lambda_{V_I}^{n-h}\right\}$, $\Lambda_{P_I} = \mathrm{diag}\left\{\Lambda_{P_I}^1, \ldots, \Lambda_{P_I}^{n-h}\right\}$, $\Lambda_{II} = \mathrm{diag}\left\{\Lambda_{II}^1, \ldots, \Lambda_{II}^h\right\}$ are matrices with positive gain coefficients ensuring the stability of differential equations (14).

As discussed in [17], using the Lyapunov stability theory it is possible to show that the solution of the above system of equations is asymptotically stable for positive gain coefficients. Moreover, for coefficients of matrices Λ_{V_I}, Λ_{P_I} chosen as

$$\Lambda_{V_i}^i \geq 2\sqrt{\Lambda_{P_i}^i}, \quad i = 1\ldots(n-h), \tag{15}$$

the solution is strictly monotonic. These properties imply that the mobile manipulator achieves the final desired location p_f with zero velocity, moreover, for initial non-singular configuration fulfilling mechanical limitations, the robot motion is free of singularities and fulfills constraints (6) in the course of task execution. Additionally, if the first constraint (3) is satisfied the Pfaffian phase constraints (4) are preserved during the whole robot movement.

Finally, after determining $\dot{e}_I$, $\ddot{e}_I$, $\dot{e}_{II}$ and substituting into (14), the trajectory of mobile manipulator can be written explicitly in the following form

$$\ddot{q}(t) = -\ddot{\mathcal{E}}^{-1}(q)\left(v_1(q,\dot{q}) + v_2(q,\dot{q})\right), \tag{16}$$

where

$$\mathcal{E}(q) = \begin{bmatrix} \dfrac{\partial e_I}{\partial q} \\ \mathcal{A}(q) \end{bmatrix}, \quad v_1(q,\dot{q}) = \begin{bmatrix} \dfrac{d}{dt}\left(\dfrac{\partial e_I}{\partial q}\right) \\ \dfrac{d\mathcal{A}(q)}{dt}\dot{q} \end{bmatrix},$$

$$v_2(q,\dot{q}) = \begin{bmatrix} \Lambda_{V_I}\dfrac{\partial e_I}{\partial q}\dot{q} + \Lambda_{P_I}e_I(q) \\ \Lambda_{II}\mathcal{A}(q)\dot{q} \end{bmatrix}.$$

3.2. Collision free motion

In order to take into account collision avoidance inequality constraints (7) the description of the mobile manipulator and its workspace should be provided. This paper assumes that the workspace is known and the surface of i-th obstacle is described by smooth function $S_O^i : \Re^m \to \Re$ ($S_O^i(p) = 0$ for each point p belonging to the Surface of the obstacle). In real-life applications information about the robot environment can be obtained from the sensors as a points cloud and transformed to analytical smooth functions describing the surfaces of obstacles. Examples of such solutions were given by [7, 10, 12] and a comprehensive overview of these methods was presented by [2].

In the presented work collision avoidance conditions were written using the techniques of obstacle enlargement as put forward by [20] with simultaneous discretization of surfaces describing the platform and the arm of the mobile manipulator. To this purpose, each obstacle in the workspace is enlarged by a certain positive value ϵ and the suitable discretization of robot components is determined. As shown by [5] for each $\epsilon > 0$ it is possible to choose discretization determining finite set of points P_M approximating the robot in such a way that if points from P_M do not collide with enlarged obstacles then the robot does not collide with the original obstacles. Using this approach collision avoidance conditions (7) can be expressed as a finite number of inequalities in the form of

$$S_O^i\left(p_M^j\right) - \epsilon \leq 0, \tag{17}$$

where p_M^j is a j-th point from P_M.

In order to obtain collision free motion, the method proposed in [17] was used. In this approach the accelerations of the mobile manipulator are perturbed in the neighborhood of the obstacle by the continuous perturbation pushing the robot away from the obstacle

$$\ddot{q}_O = -\varrho\left(\sum_{i=1}^{L_O}\frac{\partial\kappa_O^i\left(C_O^i(q)\right)}{\partial q} + \dot{q}\sum_{i=1}^{L_O}\kappa_O^i\left(C_O^i(q)\right)\right), \tag{18}$$

where ϱ is the positive coefficient determining the strength of the influence of perturbation, $\kappa_O^i(\cdot)$ is any continuous, differentiable interior penalty function equaling 0 outside the neighborhood of the obstacle and increasing when the robot approaches the surface of the obstacle. It is worth noting that the first component of the dependency is responsible for pushing the robot away from the obstacle, and the second one reduces the velocity of the mobile manipulator in the obstacle proximity. As it presented in [17], using the Lyapunov stability theory it is possible to show that the perturbation (18) forces the mobile manipulator to escape from the obstacle.

In order to find collision free motion the trajectory (16) should be extended with perturbation (18). It is worth noting that such a solution can disturb the robot movement only in the proximity of the obstacles, when the perturbation is active. As a result, it affects the condition (11) and may lead to the decrease in the manipulability measure, however, it can only occur near the obstacle surface, when the change of the configuration is necessary to avoid the collision. Additionally, in order to prevent the violation of nonholonomic constraints the use of the projection operator onto the null space of the matrix $\mathcal{A}$ is proposed. Finally, the collision-free trajectory of the mobile manipulator is described by the dependency

$$\ddot{q}(t) = -\mathcal{E}^{-1}(q)\left(v_1(q,\dot{q}) + v_2(q,\dot{q})\right) + \left(I - \mathcal{A}^{\dagger}\mathcal{A}\right)\ddot{q}_O, \tag{19}$$

where I is $(n \times n)$ the identity matrix and $\mathcal{A}^{\dagger} = \mathcal{A}^{\mathrm{T}}(\mathcal{A}\mathcal{A}^{\mathrm{T}})^{-1}$ is the pseudoinverse of the matrix $\mathcal{A}$.

It should be noted that the presented method if of a local character so it is possible to stuck in the local minima or saddle points. This disadvantage can be overcome by applying small perturbation if the mobile manipulator stops before reaching the final point. Such an algorithm, for convex shaped obstacles, was presented in [11]. The authors suggested perturbation forcing the motion of the robot along any of the basis vector of the tangential hyperplane of the obstacle boundary. As was shown, such an approach ensures leaving a saddle point in one iteration and it should be repeated several times if the mobile manipulator is stuck in the local minima.

4. Control constraints

The trajectory (19) considers all the conditions listed in Section 2, except the control constraints (8) resulting from capabilities of robot actuators. As was shown in previous works by the authors [16, 17] the control limitations can be considered by a suitable choice of gain coefficients Λ_{V_l} and Λ_{P_l}, the disadvantage of such a solution, however, is significant increase in task execution time. In order to eliminate this disadvantage, in this paper the approach of scaling the trajectory only in certain time periods is proposed in this paper. To achieve it, an additional variable, called the virtual control and affecting the trajectory only if robot controls are close to their limitations, is introduced. The preliminary idea of such an approach was presented in [15], but in this work the concept is significantly extended and supplemented with the condition for the existence of the solution.

In order to take control constraints into account, it is necessary to know the dynamic equations of the mobile robot, given in a general form as

$$M(q)\ddot{q} + c(q,\dot{q}) + \mathcal{A}^{\mathrm{T}}\lambda = B\tau, \tag{20}$$

where $M(q)$ denotes $(n \times n)$ the positive inertia matrix, $c(q,\dot{q})$ is n-dimensional vector representing Coriolis, centrifugal, viscous, Coulomb friction and gravity forces, λ is h-dimensional vector of the Lagrange multipliers corresponding to nonholonomic constraints (4) and B is $n \times (n–h))$ full rank matrix (by definition) describing which state variables of the mobile manipulator are directly driven by the actuators.

The extended Pffafian matrix $\mathcal{A}(q)$ is the full rank, so there exists the full rank $(n \times (n - h))$ matrix $N(q)$, orthogonal to $\mathcal{A}$, which satisfies the relation $\mathcal{A}(q)N(q) = 0$. Thus, the equation (20) can be left-multiplied by $N^{\mathrm{T}}(q)$ and written in the new form as

$$N^{\mathrm{T}}(q)M(q)\ddot{q} + N^{\mathrm{T}}(q)c(q,\dot{q}) = N^{\mathrm{T}}(q)B\tau. \tag{21}$$

As shown in [3] it is possible to choose the configuration of motorization for any nondegenerate nonholonomic platform which provides full platform mobility and ensures a full rank of the matrix $N^{\mathrm{T}}(q)B$, so the controls of the mobile manipulator can be determined from (21) as follows

$$\tau = \left(N^{\mathrm{T}}(q)B\right)^{-1}\left(N^{\mathrm{T}}(q)M(q)\ddot{q} + N^{\mathrm{T}}(q)c(q,\dot{q})\right). \tag{22}$$

It should be emphasized that the above transformation is necessary to determine the trajectory scaling coefficient, the remaining calculations are performed using a model expressed in generalized coordinates. Such trajectory scaling is carried out by introducing virtual control $u(t)$, which takes on values between 0 and 1, affecting the trajectory in limited periods of time, in which control signals are close to constraints. To achieve it, the virtual control $u(t)$ is introduced to trajectory (19) in such a way as not to change the character of the robot movement (the robot motion is slowed down when needed).

$$\ddot{q}(t) = -\mathcal{E}^{-1}(q)\left(v_1 + u(t)v_2\right) + u(t)\left(I_n - \mathcal{A}^{\dagger}\mathcal{A}\right)\ddot{q}_O. \tag{23}$$

Substituting (23) into (22) the robot controls can be written as a linear function of virtual control $u(t)$ as follows N

$$\tau(u) = a(q,\dot{q})u(t) + b(q,\dot{q}), \tag{24}$$

where

$$a(q,\dot{q}) = -\left(N^{\mathrm{T}}(q)B\right)^{-1} N^{\mathrm{T}}(q)M(q)\Big(\mathcal{E}^{-1}(q)v_2(q,\dot{q}) -$$

$$-\left(I_n - \mathcal{A}^{\dagger}\mathcal{A}\right)\ddot{q}_O\Big),$$

$$b(q,\dot{q}) = -\left(N^{\mathrm{T}}(q)B\right)^{-1} N^{\mathrm{T}}(q)\left(M(q)\mathcal{E}^{-1}(q)v_1(q,\dot{q}) - c(q,\dot{q})\right).$$

Due to the inaccuracy of the robot dynamic model the safety zones of size determined by $\varepsilon_\tau \in (0,1)$ for $\tau_{\min}$ and $\tau_{\max}$ are introduced as follows

$$\begin{aligned}\tau_{\varepsilon,\min} &= \tau_{\min} + 0.5\varepsilon_\tau\left(\tau_{\max}-\tau_{\min}\right)\\ \tau_{\varepsilon,\max} &= \tau_{\max} - 0.5\varepsilon_\tau\left(\tau_{\max}-\tau_{\min}\right),\end{aligned} \tag{25}$$

The trajectory of the mobile manipulator is scaled when any control exceeds $\tau_{\varepsilon,\min}$ or $\tau_{\varepsilon,\max}$, which maintains a certain margin enabling the control systems to introduce corrections to the trajectory being realized. Finally, using dependency (24) the control constraints (8) can be written in the new form as

$$\tau_{\varepsilon,\min} \le a(q,\dot q)u(t) + b(q,\dot q) \le \tau_{\varepsilon,\max} \tag{26}$$

According to the proposed method, the virtual control $u(t)$ takes a value equal to 1 when the control signals of the mobile manipulator are within the range determined by the dependencies (25). In this case, the trajectory is not scaled and the robot movement follows the original solution described by the dependency (23). If, at a given time instant, controls exceed the safety margins (25), it is necessary to find the $\hat u$ value to satisfy constraints (26). Hence, for each i-th control that exceeded its limit, value $\hat u_i$ should be determined in such a way as to satisfy the inequality

$$\tau^i_{\varepsilon,\min} \le a^i\hat u_i + b^i \le \tau^i_{\varepsilon,\max}, \tag{27}$$

where a^i, b^i are i-th elements of vectors $a(q,\dot q)$ and $b(q,\dot q)$.

To find the value $\hat u_i$, it is assumed that the coefficient a^i is non-zero and four cases are considered

$$\text{(a)}\ \ \tau^i > \tau^i_{\varepsilon,\max} \quad \text{and} \quad a^i > 0:\ \ \hat u_i \le \frac{\tau^i_{\varepsilon,\max} - b_i}{a_i},$$

$$\text{(b)}\ \ \tau^i < \tau^i_{\varepsilon,\min} \quad \text{and} \quad a^i < 0:\ \ \hat u_i \le \frac{\tau^i_{\varepsilon,\min} - b_i}{a_i},$$

$$\text{(c)}\ \ \tau^i > \tau^i_{\varepsilon,\max} \quad \text{and} \quad a^i < 0:\ \ \hat u_i \ge \frac{\tau^i_{\varepsilon,\max} - b_i}{a_i},$$

$$\text{(d)}\ \ \tau^i < \tau^i_{\varepsilon,\min} \quad \text{and} \quad a^i > 0:\ \ \hat u_i \ge \frac{\tau^i_{\varepsilon,\min} - b_i}{a_i}.$$

If at a given time instant only one control exceeds the assumed limit, then the virtual control $\hat u$ takes the value equal to the right side of corresponding inequality (a)—(d). If several control signals do not satisfy the limits then:

- if there are only cases (a) or (b), then

$$\hat u = \hat u_{\max} = \min_{i,j}\left\{\frac{\tau^i_{\varepsilon,\max} - b_i}{a_i}, \frac{\tau^j_{\varepsilon,\min} - b_j}{a_j}\right\}, \tag{28}$$

- if there are only cases (c) or (d), then

$$\hat u = \hat u_{\min} = \max_{i,j}\left\{\frac{\tau^i_{\varepsilon,\max} - b_i}{a_i}, \frac{\tau^j_{\varepsilon,\min} - b_j}{a_j}\right\}, \tag{29}$$

- if both cases (a) or (b) and (c) or (d) occur, virtual control $\hat u$ has to satisfy dependency

$$\hat u_{\min} \le \hat u \le \hat u_{\max}. \tag{30}$$

In practice, it seems that in this case it is reasonable to choose $\hat u$ as the value closest to the virtual control determined at the previous time instant.

If there are only cases (a), (b) or (c), (d) then there is always $\hat u$ which ensures that constraints (26) are satisfied. If cases (a) or (b) and (c) or (d) occur simultaneously then the fulfillment of the inequality (30) is a condition for the existence of a solution.

At the time instants when the limits are exceeded the virtual control $u(t)$ takes values û obtained according to the algorithm presented above. If the controls $\tau(t)$ decrease, and the trajectory scaling is no longer needed, the virtual control $u(t)$ should be enlarged to its maximum value equal to 1. In order to maintain the continuity of the control $\tau(t)$, it is necessary to ensure the continuous change of the virtual control $u(t)$. In order to do so, it is assumed that the $u(t)$ increases asymptotically to its maximum value according to the dependency

$$du(t)/dt = \rho\big(1 - u(t)\big), \tag{31}$$

where $\rho > 0$ determines the convergence rate.

In order to satisfy the control constraints at the initial moment of the motion the appropriate initial value of the virtual control u_0 should be given. The dependencies (28)—(30) can be used to achieve it, but it should be noted that for initial generalized velocities equal to zero, component $b(q,\dot q)$ in (24) contains only the vector $c(q,\dot q)$ with non-zero elements related to gravity forces. Hence, $u_0 = 0$ leads to controls balancing the gravity forces. It seems reasonable to assume that control constraints should not be less than these values. As shown in numerical examples, an additional advantage of such an initial value of virtual control is to ensure a smooth start of the robotic system at the beginning of the task.

Finally, according to the proposed algorithm, $u_0 = 0$ is assumed to be the initial value of the virtual control. Then $u(t)$ is increased according to the dependency (31). If the control signals exceed the safety margins (25), a new value of $\hat u$, ensuring that the constraints are satisfied, is determined using (28)—(30). If the controls $\tau(t)$ decrease and limitations (26) are satisfied, the virtual control $u(t)$ is increased according to the dependency (31).

5. Numerical example

In order to verify the effectiveness of the proposed algorithm, computer simulations involving the mobile manipulator shown in Fig. 1, consisting of nonholonomic platform of (2, 0) class and a 3-DoF 3R holonomic manipulator working in three-dimensional task space is considered. Kinematic parameters of the robot correspond to KUKA youBot mobile platform with an arm. However, in the simulations presented below, it is assumed that the platform is (2, 0) type and the arm has only three revolute joints (the last three links of the original KUKA arm form the single link of the manipulator) and the orientation of the end-effector is ignored. Finally, the parameters of the robot used in the simulations are given as follows:

- rectangular platform 0.456 m × 0.316 m × 0.046 m with wheels of radius 0.05 m,
- manipulator with a base height 0.161 m and links: 0.033 m, 0.155 m, 0.342 m,
- mass of the platform 19.803 kg, wheel 1.4 kg,
- mass of the manipulator base 0.961 kg, links: $m_1 = 1.39$ kg, $m_2 = 1.318$ kg, $m_3 = 2.496$ kg.

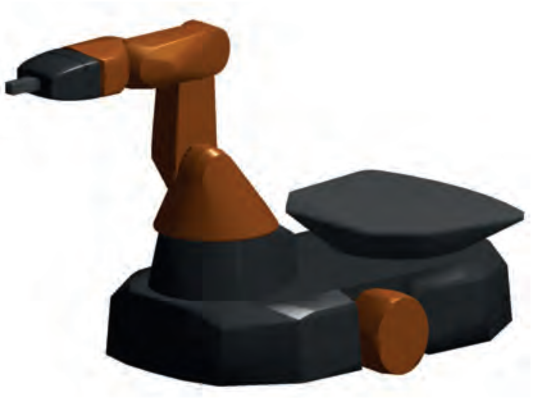

Fig. 1. Model of mobile manipulator
Rys. 1. Model mobilnego manipulatora

The vector of generalized coordinates of such mobile manipulator is described as

$$q = [x,\ \ y,\ \ \theta,\ \ \varphi_1,\ \ \varphi_2,\ \ q_1,\ \ q_2,\ \ q_3]^{\mathrm{T}},$$

and its kinematics is given as follows

$$k(q) = \begin{bmatrix} 0.17c_{\theta 123} + 0.08c_{\theta 12} + 0.03c_{\theta 1} + 0.17c_{\theta} + x \\ -0.17s_{\theta 123} - 0.08s_{\theta 12} - 0.03s_{\theta 1} + 0.17s_{\theta} + y \\ -0.34s_{23} - 0.16s_2 + 0.25 \end{bmatrix},$$

where x, y are location of the platform center, θ is the platform orientation, φ_1, φ_2 denotes the angles of driving wheels, q_1, q_2, q_3 stand for configuration angles of the manipulator joints, $c_\theta = \cos(\theta)$, $c_{\theta 1} = \cos(-\theta + q_1)$, $c_{\theta 12} = \cos(-\theta + q_1 + q_2) + \cos(\theta - q_1 + q_2)$, $c_{\theta 123} = \cos(-\theta + q_1 + q_2 + q_3) + \cos(\theta - q_1 + q_2 + q_3)$, $s_\theta = \sin(\theta)$, $s_2 = \sin(q_2)$, $s_{23} = \sin(q_2 + q_3)$, $s_{\theta 1} = \sin(-\theta + q_1)$, $s_{\theta 12} = \sin(-\theta + q_1 + q_2) - \sin(\theta - q_1 + q_2)$, $s_{\theta 123} = \sin(-\theta + q_1 + q_2 + q_3) - \sin(\theta - q_1 + q_2 + q_3)$.

The conditions (4) for the motion without lateral and longitudinal sleep, in this case, can be described as

$$\begin{bmatrix} c_\theta & s_\theta & -0.16 & -0.05 & 0 \\ c_\theta & s_\theta & 0.16 & 0 & -0.05 \\ s_\theta & -c_\theta & 0 & 0 & 0 \end{bmatrix} \begin{bmatrix} \dot{x} \\ \dot{y} \\ \dot{\theta} \\ \dot{\varphi}_1 \\ \dot{\varphi}_2 \end{bmatrix} = 0.$$

The task of the mobile manipulator is to move from non-singular, collision free configuration, fulfilling mechanical constraints

$$q_0 = [\ 0.0,\ \ -0.5,\ \ \pi/2,\ \ 0.0,\ \ 0.0,\ \ 0.0,\ \ -0.17,\ \ 0.35\ ]^{\mathrm{T}}\ \mathrm{rad}$$

to the final end-effector position

$$p_f = [\ 3.5,\ \ 4.0,\ \ 0.16\ ]^{\mathrm{T}}\ \mathrm{m},$$

maximizing the manipulability measure (5) and satisfying mechanical limitations (6):

$$q_{a,\min} = [-169\pi/180,\ -65\pi/180,\ -151\pi/180\ ]^{\mathrm{T}}\ \mathrm{rad},$$

$$q_{a,\max} = [\ \ 169\pi/180,\ \ \ 90\pi/180,\ \ \ 145\pi/180\ ]^{\mathrm{T}}\ \mathrm{rad},$$

and control limitations equal to:

$$\tau_{\min} = [-1.5,\ -1.5,\ -1.0,\ -10.0,\ -5.0\ ]\mathrm{Nm},$$

$$\tau_{\max} = [\ \ 1.5,\ \ 1.5,\ \ 1.0,\ \ \ 0.0,\ \ \ 0.0\ ]\mathrm{Nm}.$$

The mobile manipulator operates in the workspace including three obstacles:

1. cylinder: radius 0.25 m, height 0.2 m,
   base center $[0.15,\ 0.75,\ 0]^{\mathrm{T}}$m,
2. sphere: radius 0.15 m, center $[1.25,\ 0.7,\ 0.45]^{\mathrm{T}}$m,
3. cylinder: radius 0.4 m, height 0.1 m,
   base center $[1.25,\ 2.5,\ 0]^{\mathrm{T}}$m.

In order to formulate the collision avoidance conditions (17) each obstacle is enlarged by $\epsilon = 0.05$ m. The discretization of the platform and the links of the manipulator, ensuring the avoidance of the collision with the sphere and the cylinders with parameters given above, is determined as 0.14 m. Within the proposed approach the obstacles in the workspace have to be approximated by smooth surfaces. In the presented simulations solids described by superellipsoids, widely discussed by [9], are used. The parameters of superellipsoids (semidiameters a_x, a_y, a_z and coefficients χ_1, χ_2 determining the shape of the solids) representing the obstacles in the workspace are given in Tab. 1.

The sizes of neighborhoods in which perturbation affects the robot motion are equal to 0.35 m and 0.15 m for cylinders and sphere, respectively. The gain coefficients Λ used in the trajectory generator (23) are taken as

$$\Lambda_{P_I} = \mathrm{diag}(1.75,\ 1.75,\ 1.75,\ 1.75,\ 1.75),$$

$$\Lambda_{V_I} = \mathrm{diag}(2.78,\ 2.78,\ 2.78,\ 2.78,\ 2.78),$$

$$\Lambda_{II} = \mathrm{diag}(1.0,\ \ \ 1.0,\ \ \ 1.0,\ \ \ 1.0,\ \ \ 1.0).$$

Tab. 1. Parameters of superellipsoids
Tab. 1. Parametry superelipsoid

nr	a_x	a_y	a_z	χ_1	χ_2
1.	0.25 m	0.25 m	0.10 m	0.1	1.0
2.	0.15 m	0.15 m	0.15 m	1.0	1.0
3.	0.40 m	0.40 m	0.05 m	0.1	1.0

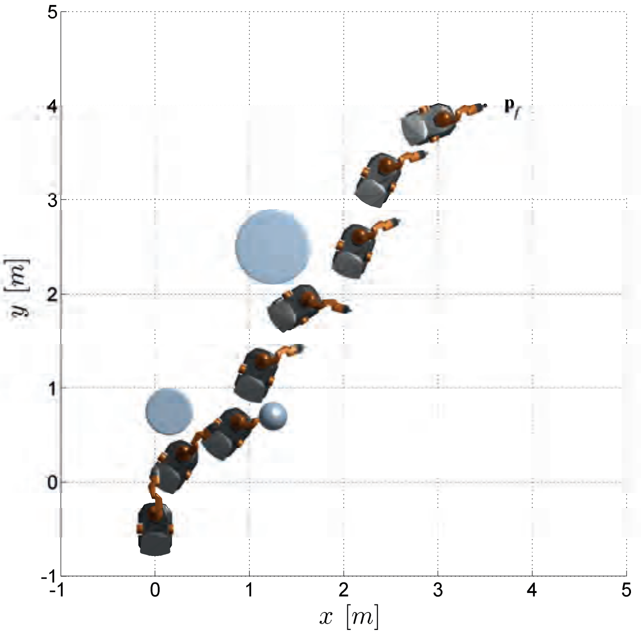

Fig. 2. Motion of mobile manipulator
Rys. 2. Ruch mobilnego manipulatora

Two cases of such a task are considered. In the first one control constraints (8) are ignored, in the other they are introduced in accordance with the approach presented in section 4. The way of performing the task in both cases is similar and it is shown in Fig. 2.

In the first case the final time of task execution is equal to 44.6 s. The minimal distance between the robot and the surface of obstacles is shown in Fig. 3. As it can be seen, this distance is greater than zero during the whole movement, so the robot motion is collision-free. The dashed horizontal lines represent the boundaries of neighborhoods surrounding the obstacles. It is evident that the robot maneuvers near obstacles most of the time, leaving the obstacles neighborhood for a short time of about 20 s and permanently in the final part of the movement. The motion in such a complex space leads to an increase in task execution time due to the second component of perturbation (18), which significantly reduces the velocity of the robot near the obstacles.

To improve readability, the values of arm joint angles are mean normalized, i.e. scaled to $[-0.5,\ 0.5]$ in order to fit in the same range, and presented in Fig. 4. As it can be seen, mechanical constraints are satisfied and joint angles remain far away from their limitations (dashed red horizontal lines represent normalized limitations).

The analysis of changes in the manipulability measure, presented in Fig. 5, makes it evident that the index generally increases during the task execution and the manipulator achieves the maximum dexterity after reaching the final point. However, a local decrease in manipulability can be seen at the beginning of the motion. In this case there was a potential collision of the manipulator arm with the first obstacle, which forced a significant change of configuration leading to the decrease in arm manipulability. After passing the obstacle the influence of perturbation (18) decreases and the minimization of criteria (9) ensures an increase in manipulability measure.

Mean normalized control signals obtained in the first case, when the constraints (8) were ignored, are shown in Figs. 6 and 7. It can be seen that both the torques of platform wheels and arm joints exceed the assumed limitations (dashed red horizontal lines represent normalized limitations). It is especially evident at the beginning of the movement when the robot starts from the initial location and in the neighborhoods of the obstacles. Signi-

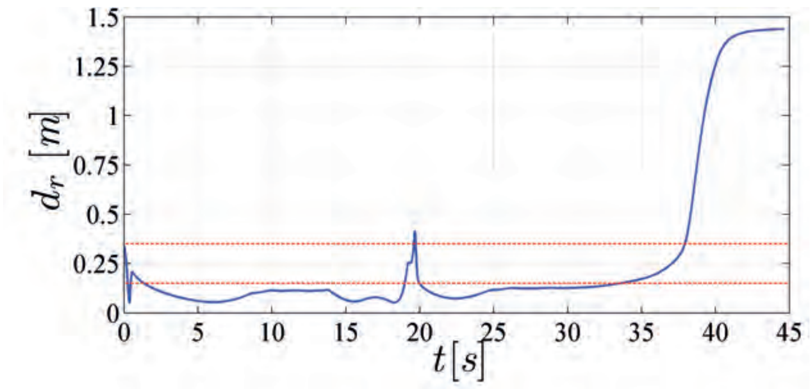

Fig. 3. Minimal distance between robot and obstacles for the first task
Rys. 3. Minimalna odległość między robotem i przeszkodami w pierwszym zadaniu

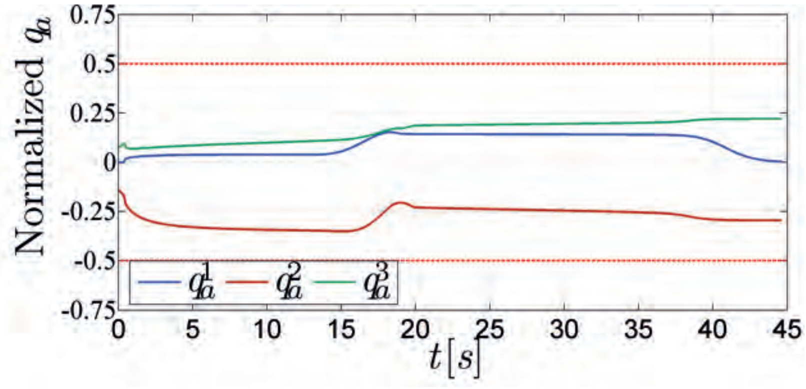

Fig. 4. Normalized arm joint angles for the first task
Rys. 4. Znormalizowane kąty konfiguracyjne ramienia w pierwszym zadaniu

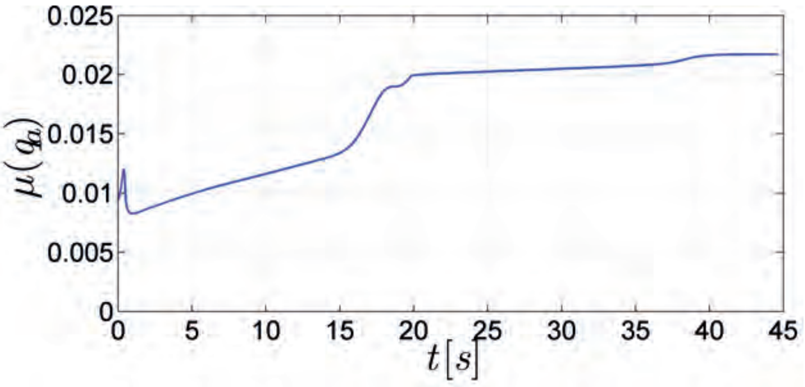

Fig. 5. Arm manipulability measure for the first task
Rys. 5. Miara manipulowalności ramienia w pierwszym zadaniu

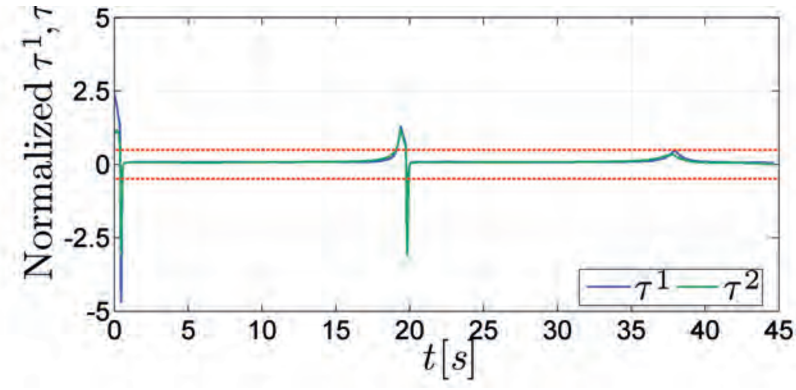

Fig. 6. Normalized wheels torques for the first task
Rys. 6. Znormalizowane momenty obrotowe kół w pierwszym zadaniu

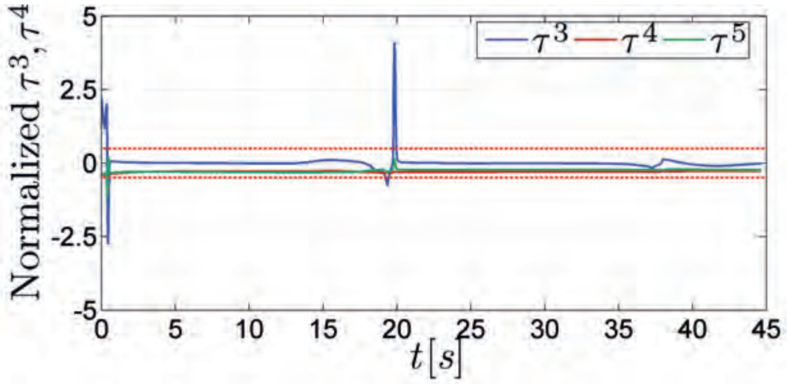

Fig. 7. Normalized arm joints torques for the first task
Rys. 7. Znormalizowane momenty obrotowe przegubów ramienia w pierwszym zadaniu

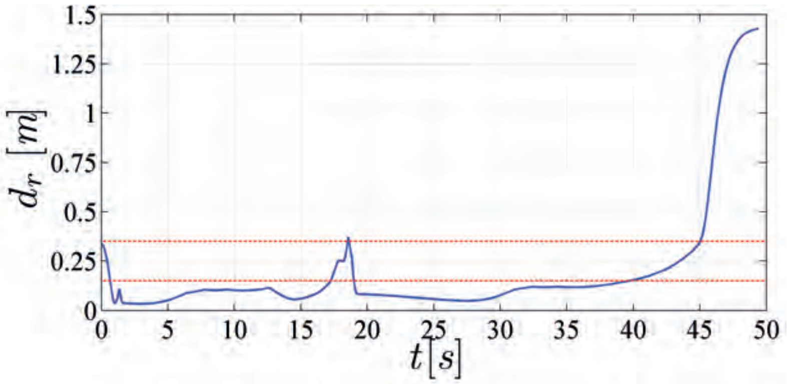

Fig. 8. Minimal distance between robot and obstacles for the second task
Rys. 8. Minimalna odległość między robotem i przeszkodami w drugim zadaniu

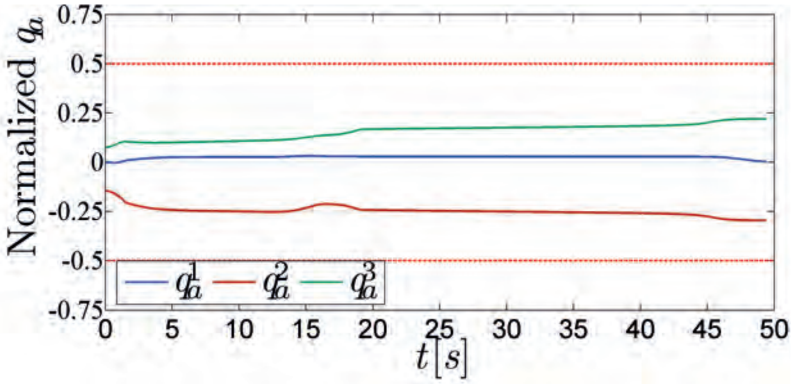

Fig. 9. Normalized arm joint angles for the second task
Rys. 9. Znormalizowane kąty konfiguracyjne ramienia w drugim zadaniu

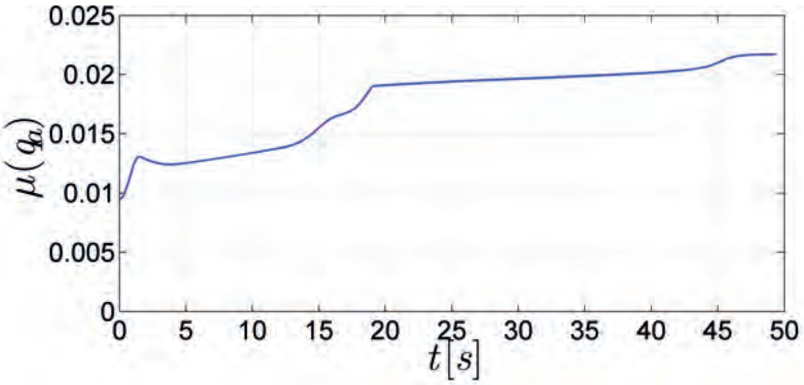

Fig. 10. Arm manipulability measure for the second task
Rys. 10. Miara manipulowalności ramienia w drugim zadaniu

ficant exceedance of the controls limits can be observed in the middle phase of the motion (18–20 s). In this stage the robot leaves the neighborhood of the second obstacle and begins to increase its velocity (wheels controls increase) and moves away from the obstacle. However, it quickly enters the safety zone of the third obstacle and, as a result, it must its reduce velocity, so the wheels controls decrease and they exceed the lower limits. Moreover, the potential collision with the robot arm exists, so it is necessary to change the first configuration angle and the corresponding control increases exceeding its limit.

In the second simulation the mobile manipulator preformed the same task as in the first case, but the control constraints were considered. The way of task execution was similar to the first simulation, however, due to the reduction of controls, the final time slightly increased to 49.4 s. For the purposes of the virtual control method, proposed in this paper, the size of safety zones for τmin and τmax was taken as $\varepsilon_{\tau} = 0.1$. The minimal distance between the robot and the obstacles, mean normalized joint angles and the manipulability measure are presented in Figs. 8–10, respectively.

Mean normalized control signals obtained in this case for platform wheels, arm joints and virtual control scaling the trajectory are shown in Figs. 11, 12 and 13, respectively. As it can be seen in Fig. 13, the value of the virtual control $u(t)$ increases at the beginning of the motion leading to increase of controls, which quickly reach safety zones of their limits. As a result, the virtual control determination algorithm, described in Section 4, is activated and virtual control $u(t)$ is modified according to dependencies (28)–(30), which results in reducing the controls in the first second of the motion. When the controls reach the safe values, the virtual control $u(t)$ begins to raise again up to a maximum value equal to 1 in accordance withe the equation (31). Similar behavior of virtual control take place in the final (about 45 s) phase of the movement.

More complex changes are visible in the middle phase (time interval 18–20 s) when the robot maneuvers between two obstacles. After changing the direction near the first obstacle (controls reach their limits, virtual control decreases) the robot continues to move (controls decrease, virtual control increases), but soon comes closer to the second obstacle and changes its direction again (controls reach their limits, virtual control decreases). Finally, as simulation results show, the use of the proposed approach allows to fulfill control limitations at the cost of a relatively small increase in execution time (about 10 %).

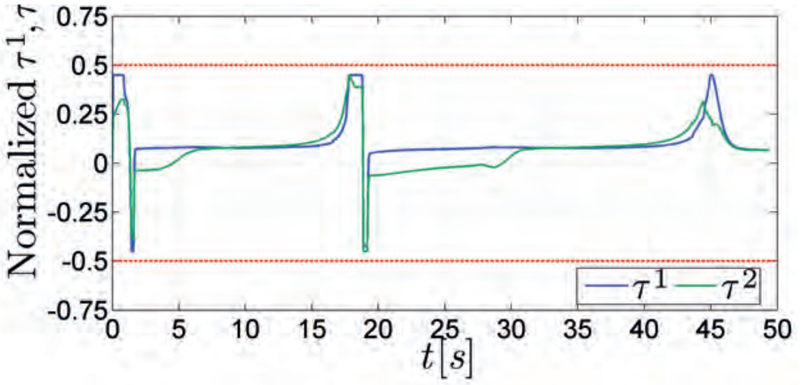

Fig. 11. Normalized wheels torques for the second task
Rys. 11. Znormalizowane momenty obrotowe kół w drugim zadaniu

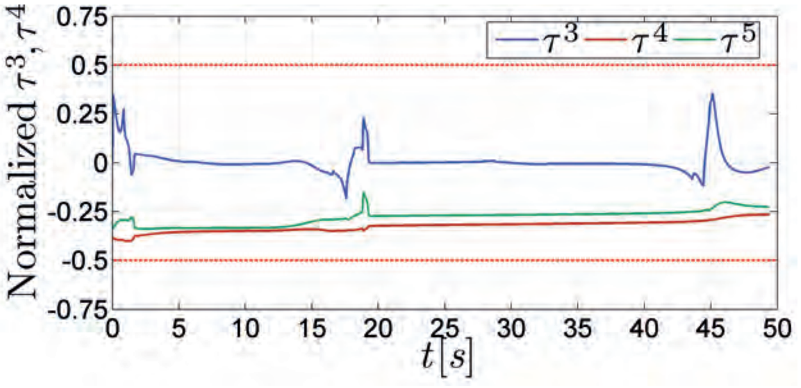

Fig. 12. Normalized arm joints torques for the second task
Rys. 12. Znormalizowane momenty obrotowe przegubów ramienia w drugim zadaniu

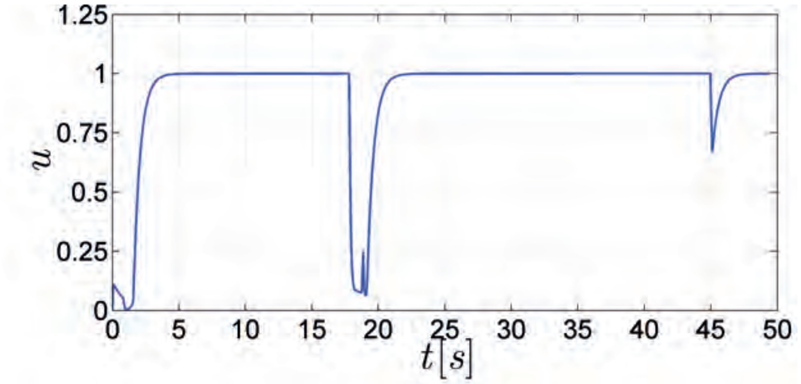

Fig. 13. Virtual control scaling trajectory for the second task
Rys. 13. Wirtualne sterowanie skalujące trajektorię w drugim zadaniu

6. Conclusion

This paper presents a method of trajectory planning when the mobile manipulator has to reach a specified end-effector position within the workspace. This approach guarantees the fulfillment of mechanical and collision avoidance constraints, additionally, it ensures the movement far away from singular configurations by maximizing the manipulability measure of the robot arm. The fulfillment of control constraints is obtained by introducing the so called virtual control scaling the trajectory in limited periods of time. As simulation results show, such an approach allows to obtain the trajectories fulfilling control constraints without significantly increasing the time of the task execution. The effectiveness of the solution is confirmed by the results of computer simulations.

References

1. Akli I., *Trajectory planning for mobile manipulators including manipulability percentage index*. „International Journal of Intelligent Robotics and Applications", Vol. 5, 2021, 543–557, DOI: 10.1007/s41315-021-00190-3.
2. Berger M., Tagliasacchi A., Seversky L.M., Alliez P., Guennebaud G., Levine J.A., Sharf A., Silva C.T. *A survey of surface reconstruction from point clouds*. „Computer Graphics Forum", Vol. 36, 2017, 301–329, Wiley Online Library.
3. Campion G., Bastin G., d'Andrea Novel B., *Structural properties and classification of kinematic and dynamic models of wheeled mobile robots*. „IEEE Transactions on Robotics and Automation", Vol. 12, No. 1, 1996, 47–62, DOI: 10.1109/70.481750.
4. Fareh R., Saad M.R., Saad M., Brahmi A., Bettayeb M., *Trajectory tracking and stability analysis for mobile manipulators based on decentralized control*. „Robotica", Vol. 37, No. 10, 2019, 1732–1749, DOI: 10.1017/S0263574719000225.
5. Galicki M., *The selected methods of manipulators' optimal trajectory planning*. WNT Publisher 2000 (in Polish).
6. Galicki M., *Task space control of mobile manipulators*. „Robotica", Vol. 29, No. 2, 2011, 221–232, DOI: 10.1017/S026357471000007X.
7. Gálvez A., Iglesias A., *Particle swarm optimization for non-uniform rational B-spline surface reconstruction from clouds of 3D data points*. „Information Sciences", Vol. 192, 2012, 174–192, DOI: 10.1016/j.ins.2010.11.007.
8. Huang Q., Tanie K., Sugano S., *Coordinated motion planning for a mobile manipulator considering stability and manipulation*. „International Journal of Robotics Research", Vol. 19, No. 8, 2000, 732–742, DOI: 10.1177/02783640022067139.
9. Jaklic A., Leonardis A., Solina F., *Segmentation and recovery of superquadrics*, Vol. 20, 2013, Springer Science & Business Media, DOI: 10.1007/978-94-015-9456-1.
10. Keller P., Kreylos O., Cowgill E.S., Kellogg L.H., Hering-Bertram M., *Construction of Implicit Surfaces from Point Clouds Using a Feature-based Approach*. „Scientific Visualization: Interactions, Features, Metaphors", Vol. 2, 2011, 129–143, Schloss Dagstuhl–Leibniz-Zentrum fuer Informatik, DOI: 10.4230/DFU.Vol2.SciViz.2011.129.
11. Khansari-Zadeh S.M., Billard A., *A dynamical system approach to realtime obstacle avoidance*. „Autonomous Robots", Vol. 32, No. 4, 2012, 433–454, DOI: 10.1007/s10514-012-9287-y.
12. Leeper A., Chan S., Salisbury K., *Point clouds can be represented as implicit surfaces for constraintbased haptic rendering*. [In:] 2012 IEEE Internatio-

nal Conference on Robotics and Automation, 5000–5005, DOI: 10.1109/ICRA.2012.6225278.

13. Li Q., Mu Y., You Y., Zhang Z., Feng C., *A Hierarchical Motion Planning for Mobile Manipulator*, „IEEJ Transactions on Electrical and Electronic Engineering”, Vol. 15, No. 9, 2020, 1390–1399, DOI: 10.1002/tee.23206.
14. Mazur A., Płaskonka J., *The Serret–Frenet parametrization in a control of a mobile manipulator of (nh, h) type.* „IFAC Proceedings Volumes”, Vol. 45, No. 22, 2012, 405–410, DOI: 10.3182/20120905-3-HR-2030.00069.
15. Pająk G., *Trajectory planning for mobile manipulators subject to control constraints.* [In:] 11th RoMoCo ’17, 117–122, DOI: 10.1109/RoMoCo.2017.8003901.
16. Pająk G., Pająk I., *Planning of a point to point collision-free trajectory for mobile manipulators.* [In:] 10th RoMoCo ’15, 142–147, DOI: 10.1109/RoMoCo.2015.7219726.
17. Pająk G., Pająk I., *Point-to-point collision-free trajectory planning for mobile manipulators.* „Journal of Intelligent and Robotic Systems”, 2016, DOI: 10.1007/s10846-016-0390-8.
18. Prasad A., Sharma B., Vanualailai J., Kumar S., *Motion control of an articulated mobile manipulator in 3D using the Lyapunov-based control scheme.* „International Journal of Control”, Vol. 95, No. 9, 2022, 2581–2595, DOI: 10.1080/00207179.2021.1919927.
19. Sandakalum T., Ang M.H. Jr., *Motion Planning for Mobile Manipulators – A Systematic Review.* „Machines”, Vol. 10, No. 2, 2022, DOI: 10.3390/machines10020097.
20. Singh S.K., Leu M.C., *Manipulator motion planning in the presence of obstacles and dynamic constraints.* „International Journal of Robotics Research”, Vol. 10, No. 2, 1991, 171–187, DOI: 10.1177/027836499101000208.
21. Tan J., Xi N., Wang Y., *Integrated task planning and control for mobile manipulators.* „International Journal of Robotics Research”, Vol. 22, No. 5, 2003, 337–354, DOI: 10.1177/0278364903022005004.
22. Yoshikawa T., *Manipulability of robotic mechanisms.* „International Journal of Robotics Research”, Vol. 4, No. 2, 1985, 3–9, DOI: 10.1177/027836498500400201.
23. Zhou S., Pradeep Y.C., Zhu M., Amezquita-Semprun K., Chen P., *Motion control of a nonholonomic mobile manipulator in task space.* „Asian Journal of Control”, Vol. 20, No. 5, 2018, 1745–1754, DOI: 10.1002/asjc.1694.

Planowanie trajektorii dla manipulatorów mobilnych z ograniczeniami na sterowania

Streszczenie: W pracy przedstawiono metodę planowania trajektorii dla manipulatorów mobilnych uwzględniającą ograniczenia wynikające z możliwości układów napędowych robota. Spełnienie ograniczeń na sterowana zostało osiągnięte poprzez wprowadzenie wirtualnego sterowania skalującego trajektorię robota w ograniczonych przedziałach czasu. Takie podejście pozwoliło na uzyskanie trajektorii spełniających ograniczenia na sterowania bez znaczącego wydłużenia czasu realizacji zadania. Zaproponowana metoda generuje sub-optymalne trajektorie maksymalizując miarę manipulowalności ramienia robota, zachowuje ograniczenia mechaniczne oraz warunki unikania kolizji i może być zastosowana do planowania trajektorii w czasie rzeczywistym. Skuteczność zaproponowanego rozwiązania została potwierdzona symulacjami komputerowymi wykonanymi z użyciem mobilnego manipulatora o parametrach odpowiadających robotowi KUKA youBot.

Słowa kluczowe: roboty mobilne, planowanie trajektorii, ograniczenia na stan, ograniczenia na sterowania, unikanie kolizji

Grzegorz Pająk, PhD Eng

g.pajak@iim.uz.zgora.pl
ORCID: 0000-0002-3649-399X

Grzegorz Pajak received PhD degree in Automatics and Robotics from Poznan University of Technology, Poland in 1998. Now he works at University of Zielona Gora. His current research interests include optimal control of dynamic systems with special focus on trajectory planning and control of mobile robots and application of artificial intelligence systems.

Iwona Pająk, PhD Eng

i.pajak@iim.uz.zgora.pl
ORCID: 0000-0002-3923-9057

Iwona Pajak received PhD degree in Automatics and Robotics from Poznan University of Technology, Poland in 2000. Now she works at University of Zielona Gora. Her current research interests include real time motion planning of mobile robots and application of artificial intelligence systems.